

An Untethered Brittle Star Robot for Closed-Loop Underwater Locomotion

Zach J. Patterson^{1*}, Andrew P. Sabelhaus¹, Keene Chin² and Carmel Majidi^{1,2}

Abstract—Soft robots are capable of inherently safer and more stable interactions with their environment since they can mechanically deform in response to unanticipated interactions. However, their complex mechanics can make operation difficult, particularly with tasks such as locomotion, and robust systems are needed for evaluating and testing new planning and control algorithms. In this work, we present the first mobile and untethered underwater crawling soft robot. PATRICK is a robotic testbed inspired by brittle stars that demonstrates closed-loop locomotion planning. PATRICK contains five soft legs actuated by a total of 20 shape-memory-alloy (SMA) wires, providing a rich variety of possible motions. This testbed is the first instance of real-time position tracking for an untethered soft crawling robot. Experiments demonstrate that a motion planner can command the robot to locomote to a goal state, given a simple set of motion primitives. This work demonstrates progress toward full autonomy of soft, mobile robotic systems.

I. INTRODUCTION

In recent years, roboticists have increasingly taken an interest in incorporating soft, flexible, and stretchable materials and structures into their designs [1] [2]. By utilizing these types of materials and structures, soft roboticists hypothesize that robots can interact with their environments more safely and stably because of their inherent deformability - a concept often referred to as morphological intelligence [3] [4]. However, robots must also be reliably controlled to accomplish useful tasks in the real world - a task made more difficult by the complexity of soft robotic systems. Soft robots make a trade off: by accepting a great deal of additional complexity and nonlinearity in their dynamics arising out of compliance, soft robots may be better able to perform with uncertainty, both in the environment and in their own state [5].

In order for soft robots to be used more broadly in task-specific applications, it is necessary to create platforms that enable the investigation of techniques for performing specified tasks reliably on soft systems. Currently, soft robots are often designed to execute one of a few given functionalities and are better suited to ad-hoc demonstrations than to testing higher level controls, planning, and learning principles [6] [7], with some notable exceptions [8] [9]. Groups such as Marchese et al [10] have begun to integrate elements of enabling autonomy from the literature on traditional robotic

systems into the field of soft robot manipulation. This work is intended as a translation of those planning and control approaches to autonomous mobile robots. Challenges with soft robot control and modeling become especially acute when we place an untethered robot into an uncertain environment with its own power source and onboard electronics and ask it to perform with a high degree of autonomy. Relatively few soft robots in the literature have attained untethered functionality and even fewer have exhibited some degree of autonomy [8] [11]–[15]. To develop truly mobile and autonomous soft robots, we must be able to construct testbeds that allow us to begin to develop intelligent behaviors that exploit the potential of the systems. These testbeds should be untethered because (i) the incorporation of batteries and electronics is nontrivial and can have dramatic impact on robot design and (ii) a cable will have a significant effect on the locomotion of the robot, especially at the mass and length scales that most soft robots operate.

In this work, we seek to create a soft robotic platform that combines complex actuator dynamics and kinematic locomotion with a rich space of possible actions. The end result is a robot that we believe has a varied enough actuation space to explore questions of autonomy and control. See Fig. 1A for an image of the robot. Low-level feedback control has been demonstrated on other soft robotic platforms [8], but our robot is able to achieve desired positions in real time (Fig. 1B), an ability that comes from the low-dimensional representation used for planning, leveraging empirical knowledge of the system dynamics within a reactive framework. It is the first mobile and untethered soft robot, to our knowledge, that is able to accomplish such a task. What follows is a presentation of this platform and some initial results of exploring its potential as a testbed.

II. ROBOT DESIGN

This work presents a set of designs for the first untethered, underwater, crawling soft robot. This robot, named PATRICK, is inspired by the brittle star (*ophiroid*). Brittle stars have five long and slender arms and are capable of a wide variety of large motions. Although they move relatively slowly, they are still capable of locomotion speeds around 2 centimeters per second [16]. Most importantly, they fit our previously specified desire for a design with simple and kinematic limb motions that can lead to a large, rich space of potential action sequences. Their omnidirectionality also makes them an attractive source of inspiration since this enables greater agility and eliminates the need to expend time and energy for turning. The following section presents

¹ Z.J. Patterson, A.P. Sabelhaus, and C. Majidi are with the Department of Mechanical Engineering, Carnegie Mellon University, Pittsburgh, PA 15213, USA {zpatters, asabelha, cmajidi}@andrew.cmu.edu. *Corresponding Author.

² K. Chin and C. Majidi are with The Robotics Institute, Carnegie Mellon University, Pittsburgh PA 15213, USA keenech@andrew.cmu.edu

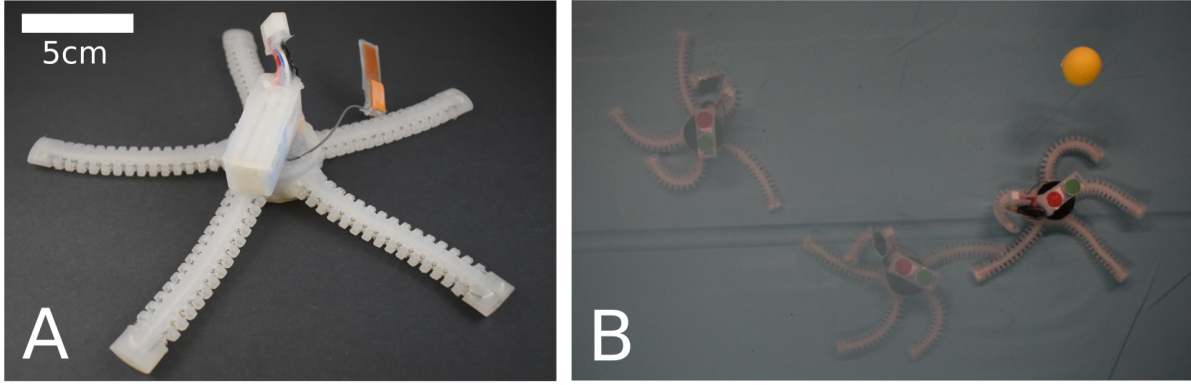


Fig. 1. (A) A Soft Underwater Untethered Brittle Star Robot named PATRICK. (B) The robot follows its goal (the yellow ball).

the design of the robot, including actuation and onboard electronics.

A. Actuator Design

To create limbs that function similarly to those of the brittle star, we chose shape memory alloy (SMA) springs (0.008in Dynalloy 90C Flexinol with a 0.054in helical diameter) as an actuator because they are lightweight and can be powered and controlled with onboard electronics and a battery. The limb design was based on the design of Walters and McGoran [17]. Each limb contains four SMA springs that are embedded in a molded silicone limb structure. The limb molds are printed with a Stratasys Objet 30 and the silicone is Smooth-On DragonSkin 10 NV silicone elastomer. The springs contract freely when current is applied and ribbed cutouts in the rubber allow the limb structure to bend as the springs contract (Fig 2A). By actuating multiple at once or in sequence, the limbs are capable of reaching a large variety of states. PATRICK has five SMA-embedded silicone limbs that are 10 centimeters long with an elliptical cross section of 1.9 by 0.9 centimeters.

B. Electronics

The robot contains power and control electronics within a central silicone hub that is sealed from water. It is controlled by a Laird BL652 module that contains a Bluetooth antenna and a nRF52832 microcontroller. The microcontroller communicates via bluetooth with an offboard nRF52832, which transmits control instructions from a computer via UART. Because the SMA limbs require high current to rapidly actuate, high powered MOSFETs are necessary to activate them with the microcontroller. We utilize SQ23 (40V) surface mount MOSFETs on breakout boards (Fig 2C). For power, the robot uses a BETA FPV 11.1V, 300mAh, 45/75C drone battery. To actuate one SMA wire, its corresponding MOSFET is pulled high and current flows through the wire, causing shape transition via Joule heating.

To construct the system, we wire the limbs to the MOSFET breakout boards which are then connected to the central control board as shown in Fig. 2B. Finally, the electronics

and limbs are cast into the central body of the robot, which is also made out of DragonSkin 10 silicone elastomer. The battery is separately sealed in silicone and placed on top of the robot, along with a cylinder of foam to get the robot close to neutral buoyancy. See Fig. 2D for a full CAD explosion. The final diameter of the robot is 25 cm and the weight of the robot is 140 grams.

III. ROBOT TESTBED

As part of this study, we created a testbed for the PATRICK robot to analyze different motions and provide closed-loop feedback. To do so, three software subsystems were created (Fig. 3A). Embedded software on PATRICK (*brittlestar_onboard*) communicates with embedded software on a microcontroller attached to a computer (*brittlestar_central*). A motion planning infrastructure built on the Robotic Operating System (ROS) and an offboard camera tracks markers on PATRICK for feedback. All software is open-source and available online¹.

A. Embedded Software

The two microcontrollers involved in PATRICK's testbed are *brittlestar_onboard* and *brittlestar_central*, both running on the same Nordic nRF52832 system. The software for *central* serves as a bridge between a USB serial port on the computer, sending and receiving strings of commands and responses over Bluetooth Low Energy with *onboard*.

A command library was implemented that allows for activation and deactivation of each shape memory alloy (SMA) actuator on PATRICK. The *onboard* software operates each shape memory alloy actuator as a finite state machine. SMA commands are sent to PATRICK in the form of (ON, OFF) for each of the 20 actuators. By varying the amount of time each SMA is activated, the motion planning system can control the bending of each leg, in each direction. Onboard safety timers trip after a timeout, deactivating each SMA if an OFF command has not been received within a time limit, preventing actuator burnout.

¹<https://github.com/softmachineslab/brittlestar>

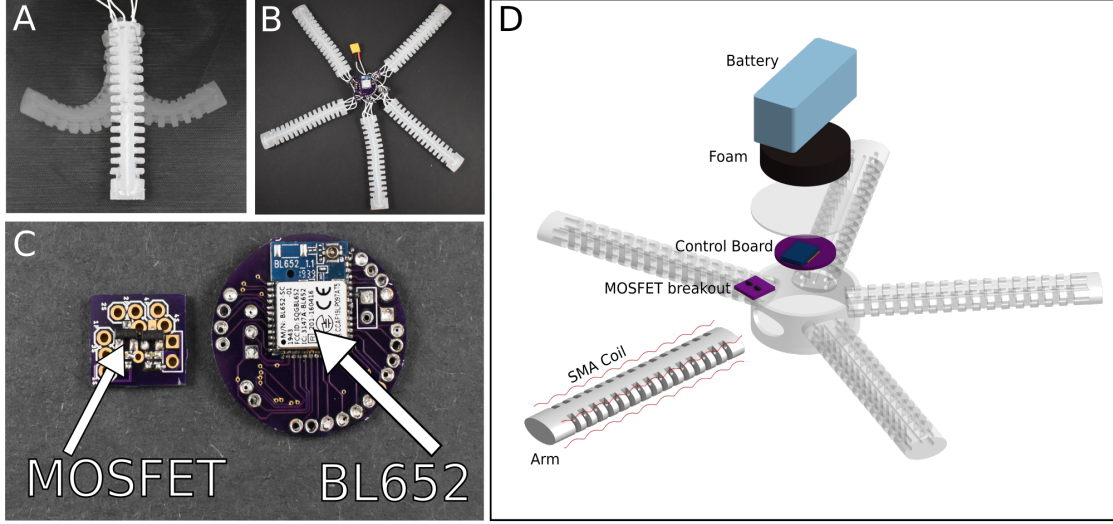


Fig. 2. (A) Brittle star robot limb with SMA actuators. (B) Robot electronics and limbs before sealing into the central silicone hub. (C) Onboard system electronics including the microcontroller PCB and a MOSFET breakout board (5X). (D) System subcomponents from top to bottom: battery, foam for neutral buoyancy, control PCB, MOSFET breakout PCB, SMA spring, silicone arm.

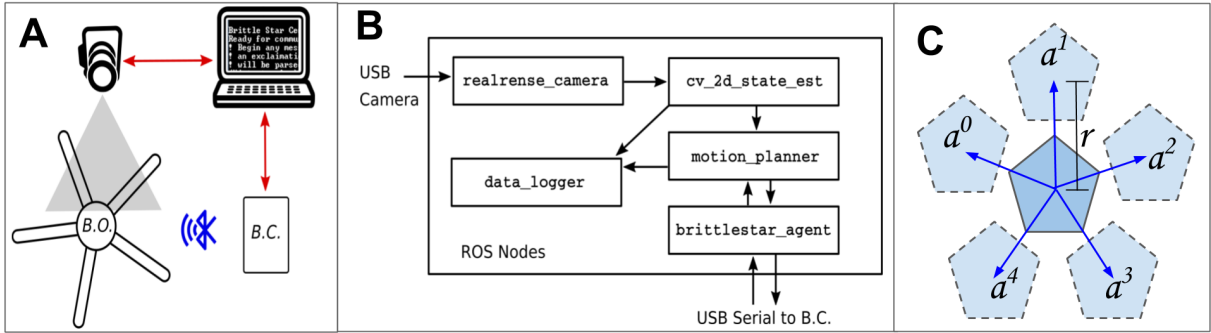


Fig. 3. (A) System architecture for PATRICK and its testbed. A camera, pointed at the robot, tracks various markers via OpenCV running on a connected computer. Embedded software on the robot ("Brittlestar Onboard") communicates over Bluetooth Low Energy to similar software running on a separate board ("Brittlestar Central") for communication over USB (red) to various ROS nodes on the computer. (B) Architecture for the various nodes used in the Robotic Operating System (ROS) package for the PATRICK robot. The Intel RealSense camera package supplies frames, then four separate nodes perform state estimation from markers on the robot, motion planning, data logging, and communication with the robot itself. Commands are sent to and from the hardware robot via the *brittlestar_central* microcontroller attached over a USB serial port. (C) The idealized state transition model used by the planner.

B. ROS Infrastructure for Robot Tracking and Communication

Alongside the flexible communication framework for PATRICK, an infrastructure of packages within the Robotic Operating System (ROS) was created that allow for visual tracking and executing motion plans. Though the camera is offboard the robot, this is the first example of any high-level closed-loop locomotion control of a completely untethered underwater soft robot.

There are five ROS nodes running on the attached computer: camera frame capture, state estimation via OpenCV, motion planning, data logging, and communication with PATRICK via *brittlestar_central* (Fig. 3B). The camera, an Intel RealSense, has a manufacturer-supplied ROS node. The remaining four are written specifically for PATRICK.

Here, we use a simple two-dimensional rigid body approx-

imation for PATRICK, calculated by tracking two colored dots on the robot (Sec. IV-B). The position and orientation of its body are represented in 2D space based on the detection of these markers. The *motion_planner* node takes these state estimates, as well as a set of possible actions from the *brittlestar_agent* (Sec. IV-A), and selects one action to send to the agent. The agent itself sends ON/OFF commands over USB serial to *central* based on the desired action.

A test procedure consists of a camera calibration, then execution of a given motion plan. Here, a second set of markers are placed on the floor of PATRICK's environment, and using them, a transformation is automatically calculated between the frame of the camera and the world frame.

IV. CLOSED-LOOP LOCOMOTION PLANNING

To demonstrate proof-of-concept closed-loop locomotion of PATRICK within its testbed, the motion planning frame-

work was implemented as a search over a set of hand-tuned motion primitives. The following section gives the two-dimensional model that was used, the chosen representation of the motion primitives, as well as the greedy planning algorithm that was then used for hardware experiments in Sec. V.

A. Motion Primitives

PATRICK exhibits a rich set of dynamics based on its 20 actuators distributed across 5 limbs. The underlying mechanics include both soft material deformation and thermal dynamics of shape-memory alloys, which are highly coupled and nonlinear. This work instead chooses a low-dimensional representation of PATRICK's state and actuation space, representing actions as combinations of inputs, as is often used for computational efficiency in the search-based planning community [18]. The following section describes the model that was used, as well as the motion primitives which were discovered. The inherent robustness of PATRICK's soft limbs allows for successful locomotion despite the low-dimensional model.

The two colored trackers on PATRICK allow for determining the position and orientation of its body in the global frame. Together, with the SMA inputs at each timestep, the robot's model is

$$\mathbf{x}_t = [x, y, \theta], \quad \mathbf{u}_t \in \{0, 1\}^{20},$$

where each of the 20 SMAs is activated or deactivated. The goal state of the robot is represented in-plane as $\bar{\mathbf{x}} = [\bar{x}, \bar{y}]$, designated by a third colored marker in the test environment. The cost functions in Sec. IV-B do not currently weigh the θ state of the robot.

For motion planning, a higher-level abstraction of the input space is used. A sequence of inputs are taken as an *action*, equivalently a *motion primitive*, over a time from t to $t + T$,

$$\mathbf{a}_t = [\mathbf{u}_t, \mathbf{u}_{t+1}, \dots, \mathbf{u}_{t+T}].$$

The transition model from \mathbf{x}_t to \mathbf{x}_{t+1} is taken with respect to actions \mathbf{a}_t , not sampling time, and is represented as an unknown function

$$\mathbf{x}_{t+1} = \mathbf{x}_t + F(\mathbf{x}_t, \mathbf{a}_t), \quad F(\mathbf{x}, \mathbf{a}^i) = [\Delta x^i, \Delta y^i, 0].$$

where each $\Delta x^i, \Delta y^i$ are a translation due to action i . However, state transitions are assumed in the planner to change the position of the robot, but not its orientation: $\theta_{t+1} = \theta_t$. Such an assumption is based on the ‘‘leading limb’’ theory of the biological brittle star [16], where the animal's body orientation does not change significantly during locomotion. Sec. V shows that this assumption is reasonable based on hardware data, given that the computer vision system closes the loop by re-sampling θ between each execution of the planner.

The ‘leading limb’ theory of the brittle star implies five motion primitives: one for each limb which could ‘lead’. Therefore, each $\Delta x, \Delta y$ is more easily parameterized in

polar coordinates, at even intervals of $(360/5) = 72$ degrees (Fig. 3C). For action i ,

$$[\Delta x, \Delta y] = [r^i \cos(\theta_t + \phi^i), r^i \sin(\theta_t + \phi^i)],$$

and the five actions are then each a displacement and an orientation, assuming that leg 0 is pointed along the $+Y$ axis at 90° ,

$$\begin{bmatrix} r^i \\ \phi^i \end{bmatrix} = \begin{bmatrix} r^0 & r^1 & r^2 & r^3 & r^4 \\ 90^\circ & 18^\circ & 306^\circ & 234^\circ & 162^\circ \end{bmatrix}$$

The sequence of SMA activations ($\mathbf{u}_t \dots \mathbf{u}_{t+T}$) for each motion primitive \mathbf{a}^i were hard coded after a trial and error discovery method to determine gaits that enabled linear motion across the plane. Multiple gait types were prototyped and one is presented here as the basis for our closed loop locomotion study (details for \mathbf{u} in accompanying software). Based again on the ‘leading limb’ model of the biological brittle star, the motion primitive performs a swing-stance gait of the two limbs to each side of the ‘leader’, so that each limb pushes the robot forward simultaneously. The $r^0 \dots r^4$ are arbitrarily chosen to be 5 cm in the transition model: this allows the planning framework to make predictions based on direction, to a reasonable level of noise on the computer vision system. Sec. V evaluates the true r^i for each of the five leading-limb primitives, data given in Fig. 4B.

B. Motion Planning with Feedback

Given a hard-coded set of possible actions and predicted transitions, a search-based motion planning algorithm was implemented for PATRICK to follow a greedy policy towards its goal. The `brittlestar_agent` node stores a list of possible actions, $\mathbf{a}_t \in \mathcal{A} = \{\mathbf{a}^0, \dots, \mathbf{a}^4\}$ for this 5-action library. Algorithm 1 is this policy, using feedback in the form of state estimates \mathbf{x}_t from the computer vision system.

The greedy policy itself is a sequential optimization over the set of motion primitives, minimizing the cost function of Euclidean distance to the goal, $\bar{\mathbf{x}}$, as in

$$c(\mathbf{x}_t) = \|\mathbf{x}_t - \bar{\mathbf{x}}\|_2.$$

The model for $F(\cdot, \cdot)$ and $\Delta x^i, \Delta y^i$ is used by the greedy algorithm to predict next states based on each action. Algorithm 1 currently uses a single-step horizon. If extended to multi-step horizon, the mismatch between the predictive model and the actual system would quickly cause the system to diverge from desired behavior, but by reevaluating at every time step, the effects of model error are minimized.

V. RESULTS

We characterized the execution characteristics of the primitives, illustrated in Fig. 4B. With the symmetric gait presented in this work, the mean distance the robot covers per iteration is 2.31 cm, and the mean execution time was 2.52 seconds. This works out to approximately 1 centimeter per second (0.04 body-lengths/s).

Results from our goal finding experiment are presented in Fig. 4A and an image of the experiment is shown in Fig. 5.

Algorithm 1: A greedy model-based policy

Input : Robot state \mathbf{x}_t , goal position $\bar{\mathbf{x}}$, set of primitives $\mathbf{a} \in \mathcal{A} = \{\mathbf{a}^0, \mathbf{a}^1, \mathbf{a}^2, \mathbf{a}^3, \mathbf{a}^4\}$, transition function $\mathbf{x}_{t+1} = \mathbf{x}_t + F(\mathbf{x}_t, \mathbf{a}_t)$, tolerance d for distance to goal

Output: Closed loop trajectory of motion primitives \mathbf{a}_t to get to the goal

```
1 while  $\|\mathbf{x}_t - \bar{\mathbf{x}}\|_2 > d$  do
2   for  $\mathbf{a}^i \in \mathcal{A}$  do
3      $\hat{\mathbf{x}}_{t+1} = \mathbf{x}_t + F(\mathbf{x}_t, \mathbf{a}^i)$ 
4      $c(\hat{\mathbf{x}}_{t+1}) = \|\hat{\mathbf{x}}_{t+1} - \bar{\mathbf{x}}\|_2$ 
5   end
6    $\mathbf{a}^t = \arg \min_{\mathbf{a}^i} c(\hat{\mathbf{x}}_{t+1})$ 
7    $\mathbf{x}_{t+1} \leftarrow \text{Robot.execute}(\mathbf{a}^t)$ 
8 end
```

The robot executes its greedy policy and moves towards the goal with a near monotonic decrease in cost. It is important to note that the distance to goal never reaches 0 because the robot runs into the goal and its arms - 10 centimeters long - prevent it from getting any closer.

VI. DISCUSSION

While PATRICK was not optimized for speed, its average velocity of 1 cm/s is comparable to the range of speeds of biological brittle stars (roughly 0.5 - 2 cm/s) [16]. It achieves this speed using the limited, unparameterized motion primitives characterized in Fig 4B. It is notable that the distance varies significantly both within each primitive and between them. The inter-limb variance is due to uncharacterized limb force output and displacement which are sensitive to differences in manufacturing. Additionally, because of the complex nature of the SMA actuators coupled with the rubber beam which comprises each limb, every actuator is itself a nonlinear dynamical system with a large amount of hysteresis. While it is tractable to model such a system with a deterministic dynamical systems model [19] [20], with DER [21] [22], or within the broad framework of geometric mechanics [23], the open-loop performance of the system is likely still not sufficient for useful, repeatable behavior.

Given this variability in limb functionality and primitive execution, it is notable that PATRICK is still able to reach the goal. This means that the strategy of closed-loop planning over high level primitives combined with the deformable platform is quite robust to uncertainty. This expressiveness is possible even in the context of the system's noisy and complicated dynamics due to the soft deformable structure's robustness to damage and the empirical, high-level approach to control. The "morphological intelligence" of these structures obviates many of the potential problems caused by variance in the execution of primitives. For rigid systems, small noise in actuation space can cause large, potentially unsafe variations in the behavior of the physical system. The continuum nature of the limbs of the soft system both reduces

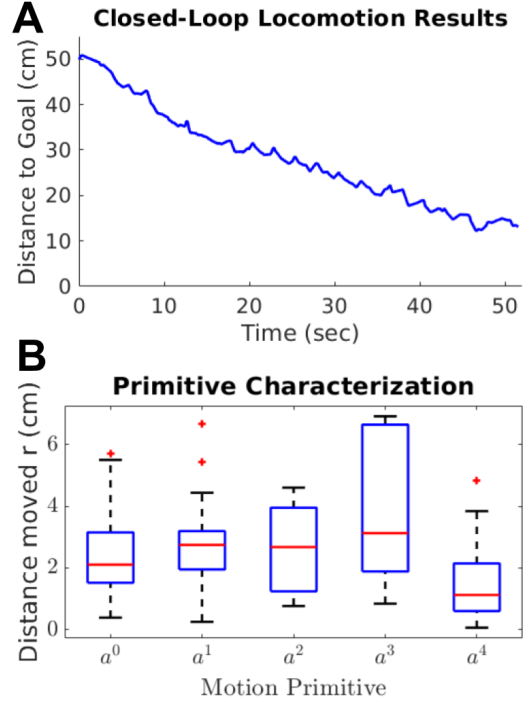


Fig. 4. (A) Movement of the robot during a representative hardware test of the goal-seeking policy, as tracked by the computer vision system. The robot moves roughly 40 cm over the course of 50 seconds to reach the goal state, stopping before collision. The greedy policy gives an almost-monotonic decrease in cost, even in hardware. (B) Characterization of the actual state transitions induced by executing the primitives.

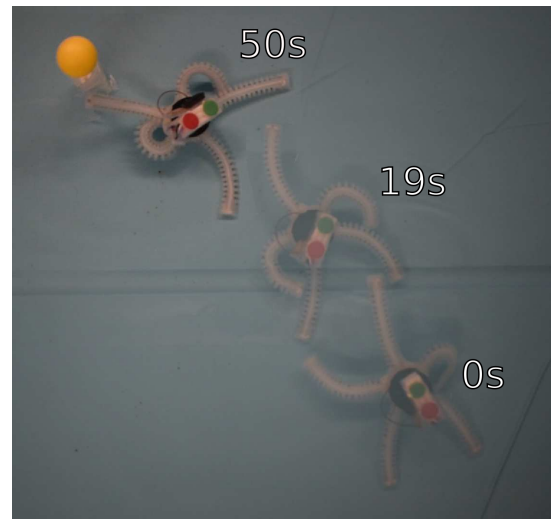


Fig. 5. Frames of the robot along its path to the goal, along with the timestamps for each image.

discontinuities in the task space evaluation of nominal primitives, as well as increases the safety of executing imprecise primitives. This demonstrates that we can produce robots that leverage complex dynamics to successfully navigate in an uncertain world without sacrificing the ability to perform useful high level tasks.

VII. CONCLUSIONS AND FUTURE WORK

We have presented PATRICK, a soft robotic brittle star and the first untethered underwater crawling robot that robustly approaches a desired location using feedback control. By iteratively planning over high-level motion primitives and leveraging vision-based state feedback, enables a great degree of improvement over the open loop behavior and allows the robot to perform useful high level tasks. The system also incorporates ROS-based distributed computation, which is notable as most soft robots in the literature take a more ad-hoc approach to software infrastructure. By taking advantage of the flexibility of traditional robotics tools like ROS and Python, we enable more sophisticated behavior and systems (as demonstrated by the goal finding experiment). We believe that, taken together, these features represent a significant step forward in the development of useful autonomous soft robots, particularly for mobile applications when onboard power and control is necessary.

Future work will focus on broadening the variety of tasks that can be accomplished and developing techniques for controlling the system which take into account the specific implication of nonlinear soft structure and actuation. Due to the high dimensionality of PATRICK's actuation space, the limit on interesting behaviors becomes a matter of intelligent planning and control, rather than the limits of the platform itself. For example, using more sophisticated tactile sensing and primitives for grasping, this platform could potentially navigate to a submerged object, pick it up, and move it to another location or otherwise manipulate the object. While this is not a simple task, the physical capabilities of the system are not the limiting factor. The flexibility to serve as both manipulator and self manipulator is an uncommon one in mobile robots, and provides an interesting surface of problems to explore.

There is also much room for improvement and optimization. The limbs can be modeled, characterized, and optimized for a given application. By using statistical learning instead of a trial and error process, we can discover better motion primitives. Finally, although the use of computer vision for feedback control represents an important contribution of this work, the ultimate goal is to produce a robot that functions independently of an offboard camera. To do that, we need to redesign the robot to include on-board sensors that will enable us to close the loop both inside and outside of lab settings.

REFERENCES

- [1] C. Majidi, "Soft-matter engineering for soft robotics," *Adv. Mater. Technol.*, vol. 4, no. 2, p. 1800477, Feb. 2019.
- [2] D. Rus and M. T. Tolley, "Design, fabrication and control of soft robots," *Nature*, vol. 521, no. 7553, pp. 467–475, 2015.
- [3] R. Pfeifer and G. Gmez, "Morphological computation - connecting brain, body, and environment," in *Creating Brain-Like Intelligence: From Basic Principles to Complex Intelligent Systems*, B. Sendhoff, E. Krner, O. Sporns, H. Ritter, and K. Doya, Eds. Berlin, Heidelberg: Springer Berlin Heidelberg, 2009, pp. 66–83.
- [4] C. Paul, "Morphological computation: A basis for the analysis of morphology and control requirements," *Robotics and Autonomous Systems*, vol. 54, no. 8, pp. 619–630, 2006.
- [5] D. Trivedi, C. D. Rahn, W. M. Kier, and I. D. Walker, "Soft robotics: Biological inspiration, state of the art, and future research," *Applied bionics and biomechanics*, vol. 5, no. 3, pp. 99–117, 2008.
- [6] X. Huang, K. Kumar, M. K. Jawed, A. M. Nasab, Z. Ye, W. Shan, and C. Majidi, "Chasing biomimetic locomotion speeds: Creating untethered soft robots with shape memory alloy actuators," *Sci. Robotics*, vol. 3, no. 25, p. eaau7557, Dec. 2018.
- [7] H.-T. Lin, G. G. Leisk, and B. Trimmer, "Gogobot: a caterpillar-inspired soft-bodied rolling robot," *Bioinspiration & Biomimetics*, vol. 6, no. 2, p. 026007, 2011.
- [8] R. K. Katzschmann, J. DelPreto, R. MacCurdy, and D. Rus, "Exploration of underwater life with an acoustically controlled soft robotic fish," *Sci. Robotics*, vol. 3, no. 16, p. eaar3449, Mar. 2018.
- [9] M. Calisti, F. Corucci, A. Arienti, and C. Laschi, "Dynamics of underwater legged locomotion: modeling and experiments on an octopus-inspired robot," *Bioinspiration & Biomimetics*, vol. 10, no. 4, p. 046012, 2015.
- [10] A. D. Marchese, R. Tedrake, and D. Rus, "Dynamics and trajectory optimization for a soft spatial fluidic elastomer manipulator," *The International Journal of Robotics Research*, vol. 35, no. 8, pp. 1000–1019, Aug. 2015.
- [11] S. I. Rich, R. J. Wood, and C. Majidi, "Untethered soft robotics," *Nature Electronics*, vol. 1, no. 2, pp. 102–112, 2018.
- [12] X. Huang, K. Kumar, M. K. Jawed, A. M. Nasab, Z. Ye, W. Shan, and C. Majidi, "Chasing biomimetic locomotion speeds: Creating untethered soft robots with shape memory alloy actuators," *Sci. Robotics*, vol. 3, no. 25, p. eaau7557, Dec. 2018.
- [13] S. K. Mitchell, X. Wang, E. Acome, T. Martin, K. Ly, N. Kellaris, V. G. Venkata, and C. Keplinger, "An easy-to-implement toolkit to create versatile and high-performance hasel actuators for untethered soft robots," *Adv. Sci.*, vol. 6, no. 14, p. 1900178, Jul. 2019.
- [14] M. T. Tolley, R. F. Shepherd, B. Mosadegh, K. C. Galloway, M. Wehner, M. Karpelson, R. J. Wood, and G. M. Whitesides, "A resilient, untethered soft robot," *Soft Robotics*, vol. 1, no. 3, pp. 213–223, Aug. 2014.
- [15] T. Li, G. Li, Y. Liang, T. Cheng, J. Dai, X. Yang, B. Liu, Z. Zeng, Z. Huang, Y. Luo, T. Xie, and W. Yang, "Fast-moving soft electronic fish," *Sci Adv*, vol. 3, no. 4, p. e1602045, Apr. 2017.
- [16] H. C. Astley, "Getting around when youre round: quantitative analysis of the locomotion of the blunt-spined brittle star, ophiocomma echinata," *J. Exp. Biol.*, vol. 215, no. 11, p. 1923, Jun. 2012.
- [17] P. Walters and D. McGoran, "Digital fabrication of smart structures and mechanisms - creative applications in art and design," *NIP & Digital Fabrication Conference*, vol. 2011, no. 1, pp. 185–188, Jan. 2011.
- [18] M. Likhachev, "Search-based planning with motion primitives," 2010.
- [19] M. R. Zakerzadeh, H. Salehi, and H. Sayyaadi, "Modeling of a nonlinear euler-bernoulli flexible beam actuated by two active shape memory alloy actuators," *Journal of Intelligent Material Systems and Structures*, vol. 22, no. 11, pp. 1249–1268, Jul. 2011.
- [20] S. G. Shu, D. C. Lagoudas, D. Hughes, and J. T. Wen, *Smart Materials and Structures*, vol. 6, no. 3, pp. 265–277, 1997.
- [21] N. N. Goldberg, X. Huang, C. Majidi, A. Novelia, O. M. O'Reilly, D. A. Paley, and W. L. Scott, "On planar discrete elastic rod models for the locomotion of soft robots," *Soft Robotics*, vol. 6, no. 5, pp. 595–610, May 2019.
- [22] W. Huang, X. Huang, C. Majidi, and M. K. Jawed, "Dynamic simulation of articulated soft robots," *Nature Comm.*, 2020.
- [23] F. Renda, F. Giorgio-Serchi, F. Boyer, C. Laschi, J. Dias, and L. Seneviratne, "A unified multi-soft-body dynamic model for underwater soft robots," *The International Journal of Robotics Research*, vol. 37, no. 6, pp. 648–666, May 2018.